Electrical detection of spin accumulation and spin precession at room temperature in metallic spin valves

Jedema, F. J.; Costache, M. V.; Heersche, H. B.; Baselmans, J. J. A.; van Wees, B. J.

Published in:
Applied Physics Letters

DOI:
10.1063/1.1532753

Publication date:
2002

Electrical detection of spin accumulation and spin precession at room temperature in metallic spin valves

F. J. Jedema,[a] M. V. Costache, H. B. Heersche, J. J. A. Baselmans, and B. J. van Wees
Department of Applied Physics and Materials Science Center, University of Groningen, Nijenborgh 4, 9747 AG Groningen, The Netherlands

(Received 15 July 2002; accepted 4 November 2002)

We have fabricated a multiterminal lateral mesoscopic metallic spin valve demonstrating spin precession at room temperature (RT), using tunnel barriers in combination with metallic ferromagnetic electrodes as a spin injector and detector. The observed modulation of the output signal due to the spin precession is discussed and explained in terms of a time-of-flight experiment of electrons in a diffusive conductor. The obtained spin relaxation length $\lambda_{sf}=500$ nm in an aluminum strip will make detailed studies of spin dependent transport phenomena possible and allow one to explore the possibilities of the electron spin for new electronic applications at RT. © *2002 American Institute of Physics.* [DOI: 10.1063/1.1532753]

A new direction is emerging in the field of spintronics,[1–4] with a focus to inject spin currents, transfer and manipulate the spin information, and detect the resulting spin polarization in nonmagnetic metals and semiconductors. A first successful attempt to electrically inject and detect spins in metals dates back to 1985 when Johnson and Silsbee demonstrated spin accumulation in a single-crystal aluminum (Al) bar up to temperatures of 77 K.[5,6] In their pioneering experiments, they were able to observe spin precession of the induced nonequilibrium magnetization. However, the measured signals were extremely small (in the pV range), due to the relatively large sample dimensions as compared to contemporary technology.

In this letter, we report spin precession in a diffusive Al strip at room temperature (RT). The use of tunnel barriers at the ferromagnetic metal–nonmagnetic metal ($F/I/N$) interface and the reduced sample dimensions by 3 orders of magnitude, has increased the output signal [voltage/current (V/I)] of our device by more than 6 orders of magnitude as compared to Ref. 5. We find a spin relaxation length $\lambda_{sf}=500$ nm in the Al strip at RT, which is within a factor of 2 of the maximal obtainable spin relaxation length at RT, being limited by the electron-phonon scattering processes.[7] At lower temperatures, larger spin relaxation lengths can be obtained by reducing the impurity scattering rate, as was previously reported.[4–6]

The samples are fabricated by means of a suspended shadow mask evaporation process[8,9] and using electron-beam (e-beam) lithography for patterning. The shadow mask is made from a trilayer consisting of a 1.2 μm thick poly(methylmethacrylate) (PMMA-MA) base layer (Allresist GMBH ARP 680.10 in methoxy-ethanol), a 40 nm thick germanium (Ge) layer and on top a 200 nm thick PMMA layer (Allresist GMBH ARP 671.04 in chlorobenzene). The base and top resist layers have different sensitivities for e-beam radiation, which enables a selective exposure by varying the induced charge dose (400 μC/cm^2: both layers, 100 μC/cm^2: base layer only) by the e–beam.

In the first development step, the top layer is developed, followed by a anisotropic CF_4 dry etching to remove the exposed Ge layer. In a third (wet) development step the PMMA-MA base layer underneath the Ge layer is developed resulting in a suspended shadow mask, see the inset of Fig. 1(a).

In a last step, the top resist layer is etched away by using an oxygen plasma. After completion of the mask, a two-step shadow evaporation procedure is used to make the sample. First, we deposit an Al layer from the left- and right-hand sides [see inset Fig. 1(a)] under an angle of 25° with the substrate surface at a pressure of 10^{-6} mbar, thus forming a

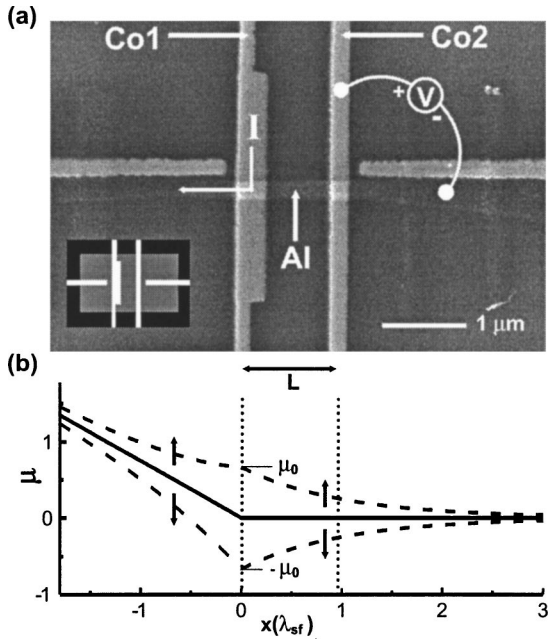

FIG. 1. (a) SEM picture of the spin valve device. The current I is injected from Co1 into the Al strip (left-hand side) and the voltage V is measured between Co2 and the Al strip (right-hand side). Inset: center of the trilayer shadow mask Black: PMMA-MA/Ge bilayer. White: SiO_2 substrate. Gray: suspended Ge layer. (b) The spatial dependence of the spin-up and spin-down electrochemical potentials (dashed) in the Al strip. The solid lines indicate the electrochemical potential (voltage) of the electrons in the absence of spin injection.

[a]Electronic mail: jedema@phys.rug.nl

continuous Al strip underneath the suspended Ge mask with a thickness of 50 nm.

Next, without breaking the vacuum, an Al_2O_3 oxide layer is formed at the Al surface due to a 10 min O_2 exposure at 5×10^{-3} mbar. In a third step, after the vacuum is recovered, a 50 nm thick cobalt (Co) film is deposited from below [see inset Fig. 1(a)] under an angle of 85° with the substrate surface. In Fig. 1(a) a scanning electron microscope (SEM) picture is shown of a sample with a Co electrode spacing of $L=1100$ nm. The conductivity of the Al and Co strips at RT were determined to be $\sigma_{Al}=1.3\times10^7\ \Omega^{-1}\,m^{-1}$ and $\sigma_{Co}=4.1\times10^6\ \Omega^{-1}\,m^{-1}$, whereas the resistance of the $Al/Al_2O_3/Co$ tunnel barriers were determined to be 800 Ω for the Co1 electrode and 2000 Ω for the Co2 electrode at RT.

In our experiment, we injected a spin polarized current ($I=100\ \mu A$) from the Co1 electrode via a tunnel barrier into the Al strip. The spin polarization P of the current is determined by the ratio of the different spin-up and spin-down tunnel barrier resistances $R_\uparrow^{TB}$ and $R_\downarrow^{TB}$, which in first order can be written as $P=(N_\uparrow-N_\downarrow)/(N_\uparrow+N_\downarrow)$.[10] Here, $N_\uparrow(N_\downarrow)$ is the spin-up (spin-down) density of states at the Fermi level of the electrons in the Co electrodes. The unequal spin-up and spin-down currents cause the electrochemical potentials $\mu_\uparrow$, $\mu_\downarrow$ of the spin-up and spin-down electrons in the Al strip to become unequal, see Fig. 1(b). The spatial dependence of $\mu_\uparrow$, $\mu_\downarrow$ can be calculated by solving the one-dimensional (1D) spin coupled diffusion equations in the Al strip.[11,12] For $x\geqslant0$, we obtain:

$$\mu(x)_\uparrow=\mu_0\exp\left(\frac{-x}{\lambda_{sf}}\right)\quad\text{and}\quad\mu(x)_\downarrow=-\mu_0\exp\left(\frac{-x}{\lambda_{sf}}\right),\tag{1}$$

where $\mu_0=eI\lambda_{sf}P/2A\sigma_N$ and $\lambda_{sf}=\sqrt{D\tau_{sf}}$, D, τ_{sf}, σ_N, and A are the spin relaxation length, diffusion constant, spin relaxation time, conductivity, and cross sectional area of the Al strip, respectively.

At a distance L from the Co1 electrode, the induced spin accumulation $(\mu_\uparrow-\mu_\downarrow)$ in the Al strip can be detected by a second Co2 electrode via a tunnel barrier. The detected potential is a weighted average of $\mu_\uparrow$ and $\mu_\downarrow$ due to the spin dependent tunnel barrier resistances:

$$\mu_F=\frac{\pm P(\mu_\uparrow-\mu_\downarrow)}{2}+\frac{(\mu_\uparrow+\mu_\downarrow)}{2},\tag{2}$$

where the $+(-)$ sign corresponds with a parallel (antiparallel) magnetization configuration of the Co electrodes. Using Eqs. (1) and (2), we can calculate the magnitude of the output signal (V/I) of the Co2 electrode relative to the Al voltage probe at distance L from Co1:

$$\frac{V}{I}=\frac{\mu_F-\mu_N}{eI}=\pm\frac{P^2\lambda_{sf}}{2A\sigma_N}\exp\left(\frac{-L}{\lambda_{sf}}\right),\tag{3}$$

where $\mu_N=(\mu_\uparrow+\mu_\downarrow)/2$ is the measured potential of the Al voltage probe. Equation (3) shows that, in absence of a magnetic field, the output signal decays exponentially as a function of L.[4]

However, in the experiment, the injected electron spins in the Al strip are exposed to a magnetic field $B_\perp$, directed perpendicular to the substrate plane and the initial direction of the injected spins being parallel to the long axes of Co electrodes. Because $B_\perp$ alters the spin direction of the injected spins by an angle $\phi=\omega_L t$ and the Co2 electrode detects their projection onto its own magnetization direction (0 or π), the spin accumulation signal will be modulated. Here $\omega_L=g\mu_B B_\perp/\hbar$ is the Larmor frequency, g is the g factor of the electron (~2 for Al), μ_B is the Bohr magneton, $\hbar$ is Planck's constant divided by 2π, and t is the diffusion time between Co1 and Co2. The observed modulation of the output signal as a function of $B_\perp$ at RT is shown in Fig. 2.

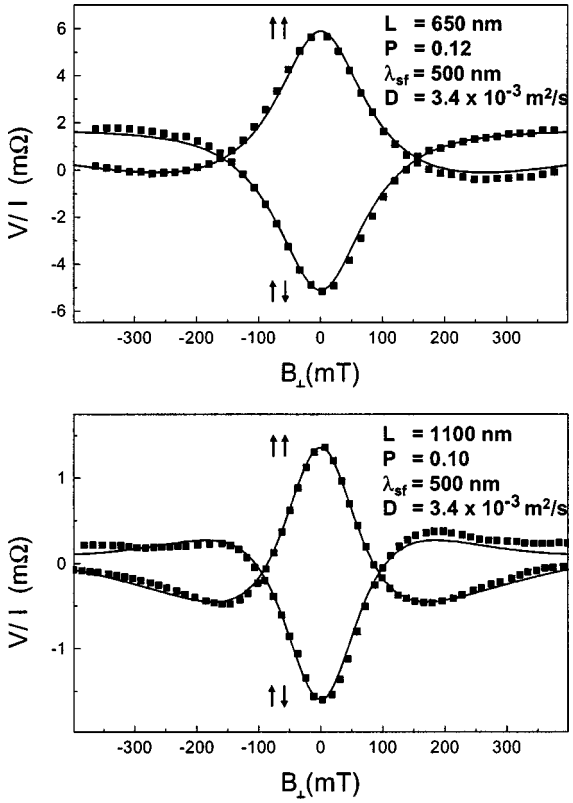

FIG. 2. Modulation of the output signal (V/I) due to spin precession as a function of a perpendicular magnetic field $B_\perp$, for $L=650$ nm and $L=1100$ nm. The solid squares represent data taken at RT, whereas the solid lines represent the best fits based on Eq. (4). We note that the fits incorporate the effect of a slight tilting of the magnetization direction of the Co electrodes out of the substrate plane (see Ref. 4).

For a parallel ↑↑ (antiparallel ↑↓) configuration, we observe an initial positive (negative) signal, which drops in amplitude as $B_\perp$ is increased from zero field. This is called the Hanle effect in Refs. 5 and 6. The parallel and antiparallel curves cross each other where the average angle of precession is about 90° and the output signal is close to zero. As $B_\perp$ is increased beyond this field, we observe that the output signal changes sign and reaches a minimum (maximum) when the average angle of precession is about 180°, thereby effectively converting the injected spin-up population into a spin-down and vice versa. We have fitted the data with Eq. (4) and using $\lambda_{sf}=500$ nm, $\sigma_N=e^2ND$, and $N=2.4\times10^{28}$ states/eV/m^3 (Ref. 13), we find the spin relaxation time $\tau_{sf}=65$ ps in the Al strip at RT to be in good agreement with theory.[14] We note that about half of the momentum scattering processes at RT is due to electron-phonon scattering, which implies that the spin relaxation length can be maximally improved by a factor of 2. A detailed discussion

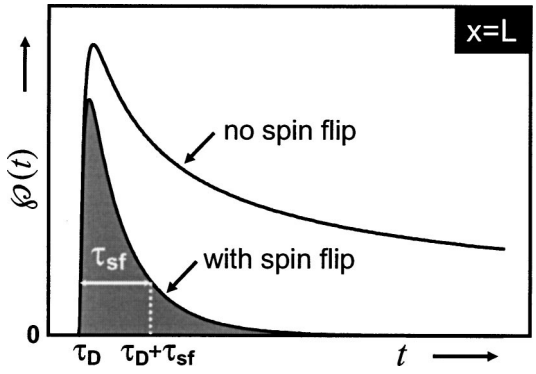

FIG. 3. Probability per unit volume that, once an electron is injected, will be present at $x=L$ without spin flip $[\wp(t)]$ and with spin flip $[\wp(t)\times\exp(-t/\tau_{sf})]$, as a function of the diffusion time t.

about spin relaxation times in nonmagnetic metallic thin films is given in Ref. 7.

Figure 2 shows the amplitude of the oscillating output signal decays with increasing $B_\perp$, caused by the diffusive nature of the Al strip. In an (infinite) diffusive 1D conductor, the diffusion time t from Co1 to Co2 has a broad distribution $\wp(t)=\sqrt{1/4\pi Dt}\times\exp(-L^2/4Dt)$, where $\wp(t)$ is proportional to the number of electrons per unit volume that, once injected at the Co1 electrode $(x=0)$, will be present at the Co2 electrode $(x=L)$ after a diffusion time t. Therefore, the output signal (V/I) is a summation of all contributions of the electron spins over all diffusion times t:

$$\frac{V(B_\perp)}{I}=\pm\frac{P^2}{e^2N(E_F)A}\int_0^\infty\wp(t)\cos(\omega_L t)\exp\left(\frac{-t}{\tau_{sf}}\right)dt. \tag{4}$$

In Fig. 3, $\wp(t)$ is plotted as a function of t, showing that long diffusion times t $(t\gg\tau_D)$ still have a considerable weight. Here $\tau_D=L^2/2D$ corresponds to the peak position in $\wp(t)$ $(\delta_\wp(t)/\delta t=0)$. So even when τ_{sf} is infinite, the broadening of diffusion times will destroy the spin coherence of the electrons present at Co2 and, hence, will lead to a decay of the output signal. However, a sign reversal of the output signal is still observed because only the electrons present at Co2 carrying their spin information are relevant. The exponential factor in the integral of Eq. (4), describing the effect of the spin–flip scattering, will cut off the diffusive broadening of $\wp(t)$ and create a window of diffusion times from τ_D to $\tau_D+\tau_{sf}$, see Fig. 3. The condition to observe more than a half period of modulation imposes $\phi_{\text{ave}}=\omega_L\tau_D\geqslant\pi$, whereas a limitation on the diffuse broadening imposes the condition $\Delta\phi=\omega_L\tau_{sf}\leqslant\pi$. Using $\tau_D=L^2/2D$, we find with this simplified picture that the requirement in order to observe at least half a period of oscillation is approximately given by: $L\geqslant\sqrt{2}\lambda_{sf}$.

Using the program MATHEMATICA, we can solve the integral $\text{Int}(B_\perp)=\int_0^\infty\wp(t)\cos(\omega_L t)\exp(-t/\tau_{sf})dt$ and we find:

$$\text{Int}(B_\perp)=\text{Re}\left(\frac{1}{2\sqrt{D}}\frac{\exp\left[-L\sqrt{\frac{1}{D\tau_{sf}}-i\frac{\omega_L}{D}}\right]}{\sqrt{\frac{1}{\tau_{sf}}-i\omega_L}}\right). \tag{5}$$

Equation (5) shows that, in the absence of precession $(B_\perp=0)$, the exponential decay of Eq. (3) is recovered. It can be shown by using standard goniometric relations that Eq. (5) is identical to the solution describing spin precession obtained by solving the Bloch equations with a diffusion term.[6] In particular, we find $\text{Int}(B_\perp)=\frac{1}{2}(\sqrt{\tau_{sf}}/2D)\times F_1\{b,l\}$, where $F_1\{b,l\}$ is derived in Ref. 6, $b\equiv\omega_L\tau_{sf}$ is the reduced magnetic field parameter and $l\equiv\sqrt{L^2/2D\tau_{sf}}$ is the reduced injector–detector separation parameter.

To conclude, we have demonstrated spin precession in an Al strip at RT. As a final note, we believe that our obtained value $P\approx10\%$ (Ref. 15) is too low and we anticipate that the output signal of our device can be improved by more than an order of magnitude by improving the material properties of the Co material.[16]

The authors wish to thank the Stichting Fundamenteel Onderzoek der Materie (FOM) and NEDO (project ''Nanoscale control of magnetoelectronics for device applications'') for financial support.

[1] *Semiconductor Spintronics and Quantum Computation*, Springer Nanoscience and Technology Series edited by D. D. Awschalom, D. Loss, and N. Samarth (Springer, New York, 2002).
[2] S. A. Wolf, D. D. Awschalom, R. A. Buhrman, J. M. Daughton, S. von Molnár, M. L. Roukes, A. Y. Chtchelkanova, and D. M. Treger, Science **294**, 1488 (2001).
[3] F. J. Jedema, A. T. Filip, and B. J. van Wees, Nature (London) **410**, 345 (2001).
[4] F. J. Jedema, H. B. Heersche, A. T. Filip, J. J. A. Baselmans, and B. J. van Wees, Nature (London) **416**, 713 (2002).
[5] M. Johnson and R. H. Silsbee, Phys. Rev. Lett. **55**, 1790 (1985).
[6] M. Johnson and R. H. Silsbee, Phys. Rev. B **37**, 5326 (1988).
[7] F. J. Jedema, M. Nijboer, A. T. Filip, and B. J. van Wees, Phys. Rev. B (to be published).
[8] G. J. Dolan, Appl. Phys. Lett. **31**, 337 (1977).
[9] L. D. Jackel, R. E. Howard, E. L. Hu, D. M. Tennant, and P. Grabbe, Appl. Phys. Lett. **39**, 268 (1981).
[10] M. Julliere, Phys. Rev. Lett. **54**, 224 (1975).
[11] P. C. van Son, H. van Kempen, and P. Wyder, Phys. Rev. Lett. **58**, 2271 (1987).
[12] T. Valet and A. Fert, Phys. Rev. B **48**, 7099 (1993).
[13] D. A. Papaconstantopoulos, *Handbook of the Band Structure of Elemental Solids* (Plenum, New York, 1986).
[14] J. Fabian and S. Das Sarma, Phys. Rev. Lett. **83**, 1211 (1999).
[15] R. Meservey and P. M. Tedrow, Phys. Rep. **238**, 173 (1994).
[16] W. F. Egelhoff, Jr., P. J. Chen, C. J. Powell, M. D. Stiles, R. D. McMichael, C.-L. Lin, J. M. Sivertsen, J. H. Judy, K. Takano, A. E. Berkowitz, T. C. Anthony, and J. A. Brug, J. Appl. Phys. **79**, 5277 (1996).